Interaction of Formamide with the Ru(001)-p(1×2)-O Surface

J. E. Parmeter,† U. Schwalke,‡ and W. H. Weinberg*

Contribution from the Division of Chemistry and Chemical Engineering, California Institute of Technology, Pasadena, California 91125. *Received November 17, 1986*

Abstract: The adsorption and decomposition of formamide on a Ru(001) surface on which is present an ordered p(1×2) overlayer of oxygen adatoms have been studied with electron energy loss spectroscopy and thermal desorption mass spectrometry. Below 260 K, formamide is chemisorbed molecularly on this surface, with two different forms existing above and below 225 K, independent of coverage. The form present below 225 K bonds to the surface via an electron lone pair of the formamide oxygen atom, while the form present above 225 K bonds to the surface via electron lone pairs on both the oxygen and nitrogen atoms. Annealing to 260 K results in the partial decomposition of the chemisorbed formamide to an η^2(N,O)-NHCHO species, analogous to η^2-formates that have been identified on transition-metal surfaces and in organometallic compounds. For sufficiently high initial formamide coverages, the chemical conversions occurring at both 225 and 260 K are accompanied by some desorption of molecular formamide. The η^2(N,O)-NHCHO decomposes near 420 K, evolving H_2 and CO, and leaving nitrogen adatoms on the surface. The nitrogen adatoms recombine and desorb near 570 K, leaving the p(1×2)–O overlayer intact on the surface. Following a saturation formamide exposure, approximately 0.05 monolayer of η^2(N,O)-NHCHO forms and decomposes on this surface.

I. Introduction

At a sufficiently low surface temperature, most if not all molecular adsorbates can chemisorb without dissociation on metal surfaces. The two most common ways for this to occur are by bonding through an electron lone pair localized on one atom of the adsorbed molecule or through the rehybridization of a molecular π-bond so that the molecule is bound to the surface in a di-σ bonded configuration. The former type of bonding occurs commonly for simple oxygen- and nitrogen-containing adsorbates such as H_2O[1] and NH_3,[2] while ethylene is a prototypical example of a molecule that on most clean metal surfaces bonds to the surface through extensive rehybridization of a molecular π-bond.[3] Molecules containing both heteroatoms with electron lone pairs and one or more π-bonds are thus of interest in studying metal surface–adsorbate interactions, since it is clear that several different surface bonding configurations are possible. Previous surface studies with a number of such molecules, including formic acid,[4] acetone,[5] formaldehyde,[6] and various heterocyclic aromatic compounds,[7] have been conducted, and in all cases they have shown that the relative amounts of bonding via electron lone pairs and π-bond rehybridization are dependent upon surface temperature, surface coverage, and the nature of the surface.

The interaction of amides with well-characterized, single-crystalline metal surfaces has received virtually no attention. The only study known to us of any amide on any metal surface is a very brief account of the decomposition of *N,N*-dimethylformamide (DMF) on Pt(111),[8] in which it was reported that the decomposition of DMF on this surface proceeds primarily via the evolution of HCN into the gas phase. However, the nature of molecularly adsorbed DMF and any intermediates leading to HCN evolution were not addressed. A determination of the structure and bonding of molecularly adsorbed amides on metal surfaces is of obvious interest in view of the above discussion, since bonding to the surface could be via the electron lone pair on the nitrogen atom, via an electron lone pair on the oxygen atom, through lone pairs on both heteroatoms, or through rehybridization of the CO double bond. These four possible bonding configurations of molecularly adsorbed formamide are shown schematically in Figure 1.

Considering the variety of amide-derived ligands characterized structurally in organometallic compounds, it is also clear that amide decomposition on metal surfaces may give rise to a number of different surface intermediates. These ligands include η^1-(C)-CONHR (R = H, alkyl, or aryl),[9] η^1(N)-NHCOH,[10] η^2-(C,O)-NR_2CO,[11] η^2(N,O)-NRCRO (both chelating and bidentate

† AT&T Bell Laboratories Predoctoral Fellow.
‡ Feodor-Lynen Research Fellow of the Alexander von Humboldt Foundation.

(1) (a) Stuve, E. M.; Madix, R. J.; Sexton, B. A. *Surf. Sci.* **1981**, *111*, 11. (b) Stuve, E. M.; Madix, R. J.; Sexton, B. A. *J. Vac. Sci. Techol.* **1982**, *20*, 590. (c) Sexton, B. A. *J. Vac. Sci. Technol.* **1979**, *16*, 1033. (d) Baro, A. M.; Erley, W. *J. Vac. Sci. Technol.* **1982**, *20*, 580. (e) Andersson, S.; Davenport, J. W. *Solid State Commun.* **1978**, *28*, 677. (f) Ibach, H.; Lehwald, S. *Surf. Sci.* **1980**, *91*, 187. (g) Fisher, G. B.; Sexton, B. A. *Phys. Rev. Lett.* **1980**, *44*, 683. (h) Secton, B. A. *J. Vac. Sci. Technol.* **1980**, *94*, 435. (i) Thiel, P. A.; Hoffmann, F. M.; Weinberg, W. H. *J. Chem. Phys.* **1981**, *75*, 5556. (j) Thiel, P. A.; Hoffmann, F. M.; Weinberg, W. H. *Phys. Rev. Lett.* **1982**, *49*, 501.

(2) (a) Gland, J. L.; Sexton, B. A.; Mitchell, G. E. *Surf. Sci.* **1982**, *115*, 623. (b) Erley, W.; Ibach, H. *Surf. Sci.* **1982**, *119*, L357. (c) Sexton, B. A.; Mitchell, G. E. *Surf. Sci.* **1980**, *99*, 539. (d) Sexton, B. A.; Mitchell, G. E. *Surf. Sci.* **1980**, *99*, 523. (e) Gland, J. L.; Sexton, B. A. *J. Catal.* **1981**, *68*, 286. (f) Fisher, G. B.; Mitchell, G. E. *J. Electron Spectrosc. Relat. Phenom.* **1983**, *29*, 253.

(3) (a) Backx, C.; de Groot, C. P. M.; Biloen, P. *Appl. Surv. Sci.* **1980**, *6*, 256. (b) Backx, C.; de Groot, C. P. M. *Surf. Sci.* **1982**, *115*, 382. (c) Nyberg, C.; Tengstal, C. G.; Andersson, S.; Holmes, M. W. *Chem. Phys. Lett.* **1982**, *87*, 87. (d) Lewsald, S.; Ibach, H.; Steininger, H. *Surf. Sci.* **1982**, *117*, 342. (e) Demuth, J. E.; Ibach, H.; Lehwald, S. *Phys. Rev. Lett.* **1978**, *40*, 1044. (f) Bertolini, J. C.; Rousseau, I. *Surf. Sci.* **1979**, *83*, 531. (g) Lehwald, S.; Ibach, H. *Surf. Sci.* **1979**, *89*, 425. (h) Ibach, H.; Hopster, H.; Sexton, B. A. *Appl. Surf. Sci.* **1977**, *1*, 1. (i) Ibach, H.; Lehwald, S. *J. Vac. Sci. Technol.* **1978**, *15*, 407. (j) Baro, A. M.; Ibach, H. *J. Chem. Phys.* **1981**, *74*, 4194. (k) Steininger, H.; Ibach, H.; Lehwald, S. *Surf. Sci.* **1982**, *117*, 342. (l) Dubois, L. H.; Castner, D. J.; Somorjai, G. A. *J. Chem. Phys.* **1980**, *72*, 5234. (m) Barteau, M. A.; Broughton, J. Q.; Menzel, D. *Appl. Surf. Sci.* **1984**, *19*, 92. (n) Hills, M. M.; Parmeter, J. E.; Mullins, C. B.; Weinberg, W. H. *J. Am. Chem. Soc.* **1986**, *108*, 3554.

(4) (a) Avery, N. R.; Toby, B. H.; Anton, A. B.; Weinberg, W. H. *Surf. Sci.* **1982**, *122*, L574. (b) Toby, B. H.; Avery, N. R.; Anton, A. B.; Weinberg, W. H. *J. Electron Spectrosc. Relat. Phenom.* **1983**, *29*, 317. (c) Sexton, B. A.; Madix, R. J. *Surv. Sci.* **1981**, *105*, 177. (d) Sexton, B. A. *Surf. Sci.* **1979**, *88*, 319. (e) Sexton, B. A. *J. Vac. Sci. Technol.* **1980**, *17*, 141. (f) Avery, N. R. *Surf. Sci.* **1982**, *11/12*, 774.

(5) (a) Avery, N. R.; Weinberg, W. H.; Anton, A. B.; Toby, B. H. *Phys. Rev. Lett.* **1983**, *51*, 682. (b) Avery, N. R.; Anton, A. B.; Toby, B. H.; Weinberg, W. H. *J. Electron Spectrosc. Relat. Phenom.* **1983**, *29*, 233. (c) Avery, N. R. *Surf. Sci.* **1983**, *125*, 771.

(6) (a) Anton, A. B.; Parmeter, J. E.; Weinberg, W. H. *J. Am. Chem. Soc.* **1985**, *107*, 5558. (b) Anton, A. B.; Parmeter, J. E.; Weinberg, W. H. *J. Am. Chem. Soc.* **1985**, *108*, 1823. (c) Richter, L. J.; Ho, W. *J. Chem. Phys.* **1985**, *83*, 2165. (d) Stuve, E. M.; Madix, R. J.; Sexton, B. A. *Surf. Sci.* **1982**, *119*, 279. (e) Wachs, I. E.; Madix, R. J. *Surf. Sci.* **1979**, *84*, 375.

(7) (a) DiNardo, N. J.; Avouris, P.; Demuth, J. E. *J. Chem. Phys.* **1984**, *81*, 2169. (b) Sexton, B. A. *Surf. Sci.* **1985**, *163*, 99. (c) Demuth, J. E.; Christmann, K.; Sanda, P. N. *Chem. Phys. Lett.* **1980**, *76*, 201. (d) Demuth, J. E.; Sanda, P. N. *Phys. Rev. Lett.* **1981**, *47*, 61. (e) Avouris, P.; Demuth, J. E. *J. Chem. Phys.* **1981**, *75*, 4783. (f) Avouris, P.; Demuth, J. E. *J. Chem. Phys.* **1981**, *75*, 5953. (g) Demuth, J. E.; Avouris, P.; Sanda, P. N. *J. Vac. Sci. Technol.* **1982**, *20*, 588. (h) Demuth, J. E.; Avouris, P. *Phys. Rev. Lett.* **1981**, *47*, 61.

(8) Garwood, G. A.; Hubbard, A. T. *Surf. Sci.* **1982**, *118*, 223.

0002-7863/87/1509-5083$01.50/0

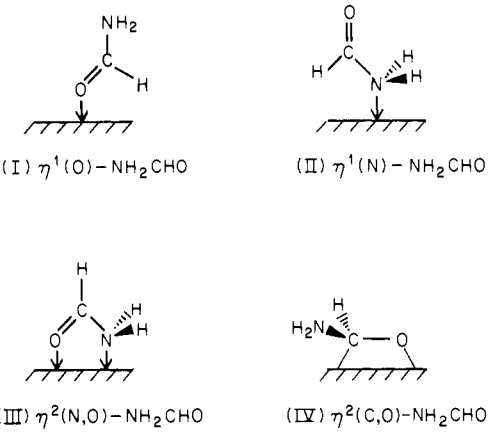

Figure 1. Schematic representation of four possible bonding configurations for formamide that is molecularly adsorbed on a metal surface. Structures I, II, and III involve bonding via heteroatom electron lone pairs, while structure IV involves bonding through rehybridization of the CO double bond. The arrows indicate lone pair donor bonds.

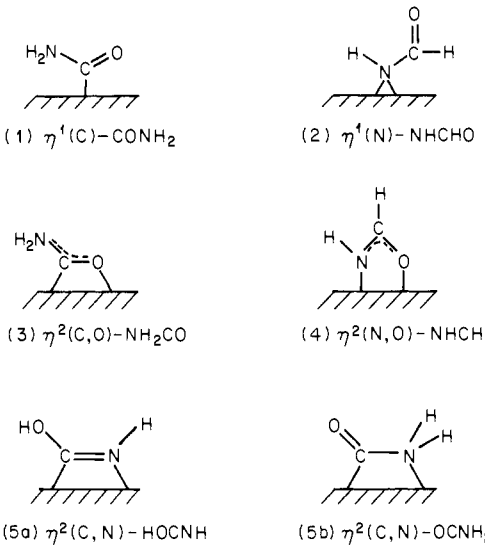

Figure 2. Several possible decomposition products of formamide on a metal surface. All of these species have known organometallic analogues (in some of which one or both hydrogens are replaced by an alkyl or aryl group).

bridging),[12] and the tautomers η^2(C,N)-HOCNR and η^2(C,N)-OCNHR.[13] The structures of these ligands are shown schematically in Figure 2 with R = H, the case that is relevant to formamide decomposition on metal surfaces. The identification

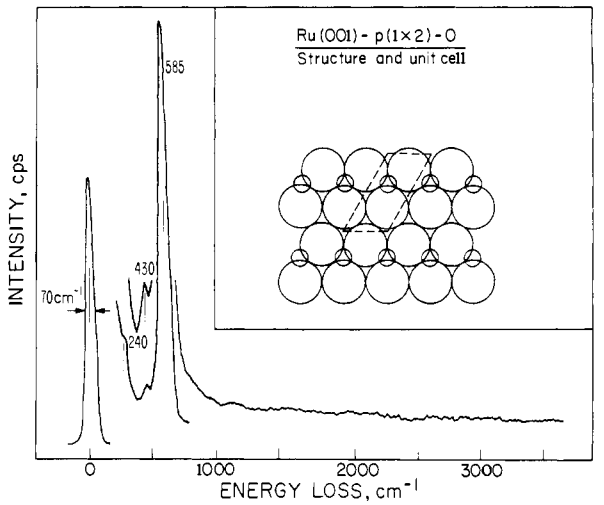

Figure 3. The EEL spectrum of the Ru(001)-p(1×2)-O surface. The inset shows the surface structure (large circle = ruthenium atom; small circle = oxygen atom) and the unit cell (dashed line). The fractional coverage of oxygen adatoms is 0.5. The loss feature at 585 cm^{-1} is magnified by a factor of 300 compared to the elastic peak, and the remainder of the EEL spectrum is magnified by a factor of 1000.

of such ligands on a metal surface is of obvious importance in establishing a relationship between the chemistry of formamide on metal surfaces and in organometallic compounds. An additional issue of fundamental importance is the degree to which the stable intermediates formed by amide decomposition on metal surfaces are related to the intermediates formed by the decomposition of related molecules such as aldehydes,[6] carboxylic acids,[4] and amines.[14]

One of the most powerful techniques for studying the structures and reactions of molecular adsorbates on single crystalline metal surfaces of low area is high-resolution electron energy loss spectroscopy (EELS),[15] especially when supplemented by thermal desorption mass spectrometry (TDMS). In this paper we present the results of an EELS and TDMS study of the interaction of the simplest amide, formamide, with a Ru(001) surface that has been modified chemically by an ordered p(1×2) overlayer of oxygen adatoms. A detailed study of the adsorption and decomposition of formamide on the clean Ru(001) surface will be presented elsewhere.[16]

The properties of the p(1×2)-O overlayer on the hexagonally close packed Ru(001) surface have been discussed in detail previously.[17] Figure 3 shows an EEL spectrum of the Ru(001)-p(1×2)-O surface, as well as the structure and unit cell of this surface. The fractional coverage of oxygen adatoms is 0.5, and they occupy threefold hollow sites exclusively. The EEL spectra of this surface show a strong peak at 585 cm^{-1} due to the ruthenium–oxygen symmetric stretching mode, with the ruthenium–oxygen asymmetric stretching mode and a ruthenium surface phonon giving rise to weaker peaks at 430 and 240 cm^{-1}, respectively. Formamide adsorption has been studied on the Ru(001)-p(1×2)-O surface as well as on the clean Ru(001) surface because the presence of the electronegative oxygen adatoms alters the electronic properties of this surface and might thus be expected to cause changes in the surface chemistry of formamide, as has been observed previously for acetone[5a] and formaldehyde[6b] adsorbed on clean and oxygen-modified Ru(001) surfaces. In addition to changing the electronic properties of the surface, the

(9) (a) Sacco, A.; Giannoccaro, P.; Vasapoloo, G. *Inorg. Chim. Acta* **1984**, *83*, 125. (b) Kruse, A. E.; Angelici, R. J. *J. Organomet. Chem.* **1970**, *24*, 231. (c) Behrens, H.; Jungbauer, A. *Z. Naturforsch.* **1979**, *34b*, 1477. (d) Lindsay, A. J.; Kim, S.; Jacobson, R. A.; Angelici, R. J. *Organometallics* **1984**, *3*, 1523.

(10) Burgess, K.; Johnson, B. F. G.; Lewis, J. *J. Chem. Soc., Dalton Trans.* **1983**, 1179.

(11) (a) Szostak, R.; Strouse, C. E.; Kaesz, H. D. *J. Organomet. Chem.* **1980**, *191*, 243. (b) Mayr, A.; Lin, Y.-C.; Boag, N. M.; Kaesz, H. D. *Inorg. Chem.* **1982**, *21*, 1704. (c) Kampe, C. E.; Boag, N. M.; Kaesz, H. D. *J. Mol. Catal.* **1983**, *21*, 297. (d) Fagan, P. J.; Manriquez, J. M.; Vollmer, S. H.; Day, C. S.; Day, V. W.; Marks, T. J. *J. Am. Chem. Soc.* **1981**, *103*, 2206. (e) Yasuda, H.; Araki, T.; Tani, H. *J. Organomet. Chem.* **1973**, *49*, 103. (f) Azam, K. A.; Yin, C. C.; Deeming, A. J. *J. Chem. Soc., Dalton Trans.* **1978**, 1201.

(12) (a) Rossi, R.; Duatti, A.; Magon, L.; Casellato, U.; Graziani, R.; Toniolo, L. *Inorg. Chim. Acta* **1983**, *74*, 77. (b) Sahajpal, A.; Robinson, R. D. *Inorg. Chem.* **1979**, *18*, 3572. (c) Schwering, H.-U.; Weidlein, J. *Chimia* **1973**, *27*, 535. (d) Jennings, J. R.; Wade, K.; Wyatt, B. K. *J. Chem. Soc. A* **1968**, 2535. (e) Adams, R. D.; Golembeski, N. M. *J. Organomet. Chem.* **1979**, *171*, C21. (f) Adams, R. D.; Golembeski, N. M.; Selegue, J. P. *Inorg. Chem.* **1981**, *20*, 1242.

(13) (a) Lin, Y. C.; Knobler, C. B.; Kaesz, H. D. *J. Am. Chem. Soc.* **1981**, *103*, 1216. (b) Kaesz, H. D.; Knobler, C. B.; Andrews, M. A.; van Bushirk, G.; Szostak, R.; Strousse, C. E.; Lin, Y. C.; Mayr, A. *Pure Appl. Chem.* **1982**, *54*, 131. The η^2(C,N)-HONCR and η^2(C,N)-OCNHR coexist as an equilibrium mixture.

(14) Baca, A. G.; Schulz, M. A.; Shirley, D. A. *J. Chem. Phys.* **1985**, *83*, 6001.

(15) (a) Ibach, H.; Mills, D. L. *Electron Energy Loss Spectroscopy and Surface Vibrations*; Academic: New York, 1982. (b) Weinberg, W. H. *Methods Exp. Phys.* **1985**, *22*, 23.

(16) Parmeter, J. E.; Schwalke, U.; Weinberg, W. H. *J. Am. Chem. Soc.*, submitted for publication.

(17) (a) Madey, T. E.; Engelhardt, H. A.; Menzel, D. *Surf. Sci.* **1975**, *48*, 304. (b) Parrott, S. L.; Praline, G.; Koel, B. E.; White, J. M.; Taylor, T. N. *J. Chem. Phys.* **1979**, *71*, 3352. (c) Rahman, T. S.; Anton, A. B.; Avery, N. R.; Weinberg, W. H. *Phys. Rev. Lett.* **1983**, *51*, 1979.

oxygen could also alter the surface chemistry of formamide by reacting directly with it to form species that cannot be formed following formamide adsorption on clean Ru(001).

II. Experimental Procedures

The EEL spectrometer and the UHV chamber housing it have been described in detail elsewhere.[18] The home-built EEL spectrometer employs 180° hemispheres as the electron energy dispersing elements both in the monochromator and the analyzer. The spectra shown in this paper were collected in the specular direction, which was 60° with respect to the surface normal, with an electron impact energy of approximately 4 eV. The resolution, defined as the full-width at half-maximum of the elastically scattered beam, varied between 70 and 90 cm^{-1}, while maintaining an elastic peak count rate of approximately 2×10^5 Hz.

The UHV chamber containing the EEL spectrometer and the Ru(001) crystal was pumped by a 220 $L \cdot s^{-1}$ Varian noble vacion pump and a titanium sublimation pump and had a working base pressure below 10^{-10} Torr. This chamber also contained a UTI-100C quadrupole mass spectrometer for thermal desorption measurements and analysis of background gases.

Liquid nitrogen cooling was employed to achieve crystal temperatures as low as 80 K. The Ru(001) crystal was cleaned with use of the well-established techniques of Ar^+ sputtering and annealing in a background of approximately 5×10^{-8} Torr of O_2.[19] Surface cleanliness was verified by both EELS and H_2 TDMS. The p(1×2)-O overlayer was prepared by exposing the clean Ru(001) surface at 80 K to 2 L of O_2 (1 L ≡ 1 Langmuir = 10^{-6} Torr·s) and annealing to 400 K. The presence of a well-ordered and complete p(1×2)-O overlayer was always verified by EELS prior to exposure of the surface to formamide at 80 K. Subsequent EEL spectra were measured after annealing to an indicated temperature and recooling to 80 K.

Formamide (99% reported purity) was obtained in the liquid state from Aldrich. It was introduced into the UHV chamber by backfilling through an UHV leak valve. The liquid formamide sample was contained in a small cell with a glass-to-metal connector, which was mounted by a miniconflat flange directly below the leak valve so that the sample-to-leak valve distance was approximately 7 in. A valve just below the miniconflat flange led via a stainless steel line to a mechanical pump so that the sample container could be evacuated after the sample was mounted. The metal tubing between the glass-to-metal seal and the leak valve was baked thoroughly and evacuated by the mechanical pump prior to all formamide exposures. Because of the high boiling point of formamide (210 °C),[20] the sample had to be heated while an exposure was being made. This was accomplished by passsing current through a wire coil wrapped around the glass sample container. During formamide exposures, the purity of the formamide was verified in situ via mass spectrometry. The principal impurity during formamide exposures was water, and, in general, the sample had to be heated several times and the metal between the sample and the leak valve had to be baked and evacuated several times before sufficiently pure formamide exposures could be achieved.

Experiments were also performed with N-deuteriated formamide, ND_2CHO, obtained from MSD Isotopes (98 atom % D). Although the ND_2CHO was always at least slightly contaminated with NDHCHO or NH_2CHO due to H/D exchange into the ND_2 group, as evidenced by NH stretching modes in the EEL spectra of ND_2CHO and its decomposition products, the EEL spectra arising from ND_2CHO exposures were nevertheless useful in helping to assign various vibrational modes. The fact that NH stretching modes appeared in multilayer EEL spectra of the ND_2CHO indicates that these modes cannot be attributed entirely to H/D exchange occuring on the Ru(001)-p(1×2)-O surface.

III. Results

A. Thermal Desorption Mass Spectrometry. Following exposure of the Ru(001)-p(1×2)-O surface to formamide at 80 K, four thermal desorption products were observed to desorb between approximately 200 and 700 K: molecular formamide (NH_2CHO), CO, H_2, and N_2. There was no detectable desorption, for example, of NH_3, H_2O, HCN, NO, H_2CO, HNCO, or CO_2. The desorption of molecular formamide and its decomposition products will be discussed separately.

1. Molecular Formamide Desorption. Figure 4 shows a series of thermal desorption spectra for molecular formamide (m/e = 45 amu) following various exposures of formamide to the Ru(001)-p(1×2)-O surface. For formamide exposures of less than approximately 1.5 L, no molecular desorption was observed, indicating that for low initial coverages all of the adsorbed formamide decomposes irreversibly on this surface. As the exposure is increased, three molecular desorption peaks appear sequentially at 255, 225, and 210 K. The lowest temperature desorption peak is quite sharp and does not saturate with increasing exposure. It may therefore be assigned unambiguously as resulting from the desorption of condensed formamide multilayers. The remaining two peaks are assigned to monolayer thermal desorption features, although the possibility that the 225 K thermal desorption feature corresponds to the desorption of second-layer formamide cannot be ruled out completely.

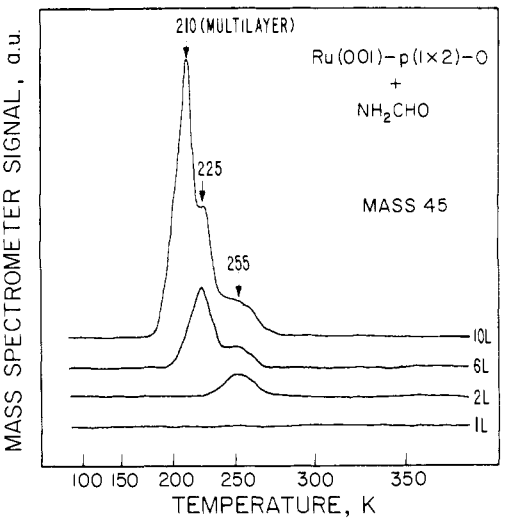

Figure 4. The molecular formamide (m/e = 45 amu) thermal desorption spectra that result following various exposures of NH_2CHO to the Ru(001)-p(1×2)-O surface at 80 K. The heating rate is approximately 8 $K \cdot s^{-1}$ in all cases.

As may be seen in Figure 4, the desorption peak at 255 K appears at lower exposures than the peak at 225 K, and neither peak displays any detectable shift in temperature as a function of coverage. This latter fact, coupled with the EELS results (cf. Section III.B) showing only molecular formamide on the surface below 260 K, indicates that both peaks result from the first-order desorption of molecular formamide, rather than from a recombinative desorption process. With use of the method of Redhead[21] and assuming a "normal" first-order preexponential factor for the rate coefficient of desorption of 10^{13} s^{-1}, the molecular adsorption states desorbing at 225 and 255 K may be assigned activation energies of desorption (heats of adsorption) of approximately 13 and 15 kcal mol^{-1}, respectively. When both states are saturated, the ratio of the amount of formamide desorbing in the 225 K peak to the amount desorbing in the 255 K peak is approximately 2:1, although there is a rather large uncertainty in this ratio due to the overlap of the two peaks. Unfortunately, there is no simple method of determining the absolute coverages of formamide desorbing in each peak. Further discussion of the nature of these two desorption states is deferred to Section IV.

2. Thermal Desorption of the Products of Formamide Decomposition: CO, H_2, and N_2. As stated above, formamide decomposition on the Ru(001)-p(1×2)-O surface results in the desorption of CO, H_2, and N_2, when the surface is annealed to 700 K. Figure 5 shows the CO (m/e = 28 amu, with a C cracking fragment at m/e = 12 amu) thermal desorption spectrum that results following a saturation formamide exposure at 80 K. A sloping background is present between 100 and 300 K due to desorption of background CO or formamide decomposition on heating wires, support leads, etc. There is a single, rather sharp desorption peak on 420 K with a small shoulder at 385 K. This shoulder is due to desorption from the surface of very small amounts (≤0.01 monolayer) of CO that is adsorbed from the chamber background, as will be discussed in Section III.B.1. The

(18) Thomas, G. E.; Weinberg, W. H. *Rev. Sci. Instrum.* **1979**, *50*, 497.
(19) Thomas, G. E.; Weinberg, W. H. *J. Chem. Phys.* **1979**, *70*, 954.
(20) Aldrich Catalog, Aldrich Chemical Co. **1984**-85, 563.
(21) Redhead, P. A. *Vacuum* **1962**, 203.

Table I. Vibrational Modes and Assignments for the Low-Temperature Form of Molecularly Chemisorbed NH_2CHO (ND_2CHO) on Ru(001)-p(1×2)-O[c]

mode	Ru(001)-p(1×2)-O NH_2CHO	Ru(001)-p(1×2)-O [ND_2CHO, ratio]	NH_2CHO(l) (26) [ND_2CHO(l), ratio]	NH_2CHO(g) (27)
$\nu_a(NH_2)$	3490	[2630, 1.33]	3330 [2556, 1.30]	3545
$\nu_s(NH_2)$	3230	[2380, 1.36]	3190 [2385, 1.34]	3451
ν(CH)	2940	[2930, 1.00]	2882 [2887, 1.00]	2852
ν(CO)	1660	[1650, 1.01]	1690 [1667, 1.01]	1734
$\delta(NH_2)$	1585	[1140, 1.39]	1608 [1118, 1.44]	1572
δ(CH)	1360	[1380, 0.99]	1391 [1398, 0.99]	1378
ν(CN)			1309 [1338, 0.98]	1255
π(CH)	n.o.	n.o.	1056 [1056, 1.00]	1030
$\rho(NH_2)$	1110	[920, 1.21]	1090 [912, 1.20]	1059
$\omega(NH_2)$	790	n.o.	750 [450, 1.67]	289
$\tau(NH_2)$	n.o.	n.o.	200	602
δ(NCO)	~525[a]	[460, 1.14]	608 [570, 1.07]	565
ν(Ru-NH_2CHO)	300[b]	[280, 1.07][b]		

[a] Overlaps with ν_s(RuO) of oxygen adatoms in the case of NH_2CHO. [b] Not resolved in the spectrum shown; sharpens with annealing to 200 K. [c] The frequency ratios $\nu(NH_2CHO)/\nu(ND_2CHO)$ are also listed in brackets following the ND_2CHO frequencies. Data for liquid phase NH_2CHO and ND_2CHO and for gas phase NH_2CHO are given for comparison. All frequencies are in cm^{-1}. n.o. = not observed, a = asymmetric, s = symmetric.

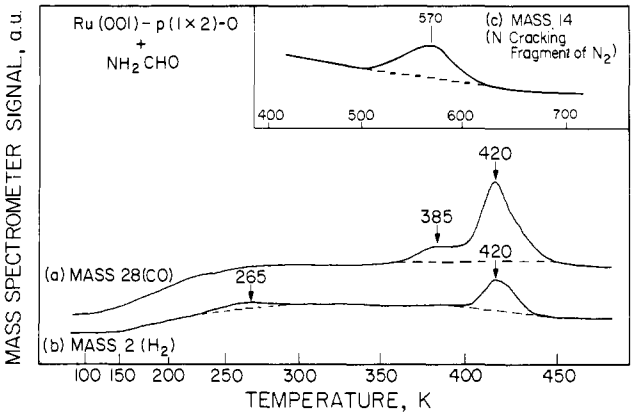

Figure 5. Thermal desorption spectra of (a) CO (m/e = 28 amu), (b) H_2 (m/e = 2 amu), and (c) (inset) N_2 (m/e = 14 amu, N cracking fragment) following a saturation NH_2CHO exposure of approximately 8 L on the Ru(001)-p(1×2)-O surface at 80 K. The heating rate is approximately 8 $K \cdot s^{-1}$ in all cases. The shoulder at 385 K in the CO spectrum is due to desorption of CO adsorbed from the chamber background. Dashed lines are approximate base lines. Note the different temperature scale in part c.

peak at 420 K is the only feature resulting from formamide decomposition on the Ru(001)-p(1×2)-O surface, and since it desorbs at a higher temperature than low coverages of CO adsorbed on Ru(001)-p(1×2)-O,[19] this is a reaction-limited desorption peak resulting from the decomposition of a surface intermediate. By comparison with thermal desorption results for CO adsorbed on clean Ru(001), where the saturation coverage is aproximately 0.68,[22] this peak is estimated to correspond to approximately 0.05 monolayer of CO. Since the only observed decomposition reaction of formamide on the Ru(001)-p(1×2)-O surface is to CO, H_2, and nitrogen adatoms, this corresponds to the fractional coverage of formamide that decomposes on this surface following a saturation exposure.

Figure 5 shows the H_2 (m/e = 2 amu) thermal desorption spectrum that results following a saturation formamide exposure on the Ru(001)-p(1×2)-O surface at 80 K. Again, a peak is observed at 420 K. The fact that this peak is coincident with the CO desorption peak at 420 K suggests strongly that both peaks result from the decomposition of the same surface species. There is also a weak maximum near 265 K, which is reproducibly above background. Better resolution of this desorption state, which contains only approximately 0.05 monolayer of hydrogen adatoms, was not possible with our experimental apparatus. However, H_2 desorption is expected at this temperature, since EEL spectra provide clear evidence for NH bond cleavage at 260 K and hydrogen has been observed not to chemisorb on Ru(001)-p(1×2)-O under UHV conditions.[6b]

Desorption of molecular nitrogen (m/e = 28 amu, with an N cracking fragment at m/e = 14 amu) occurs between approximately 520 and 630 K, with a maximum desorption rate at approximately 570 K. A mass 14 thermal desorption spectrum is shown in the inset of Figure 5. The desorption of N_2 in this temperature range results from the recombinative desorption of nitrogen adatoms, because molecularly chemisorbed N_2 on both clean and oxygen precovered Ru(001) surfaces desorbs well below 200 K.[23] The fact that no desorption of NO occurs as a result of the combination of nitrogen and oxygen adatoms is in agreement with previous studies of NO[24] and NO_2[25] adsorption and decomposition on Ru(001).

B. Electron Energy Loss Spectroscopy. In discussing the EELS results for formamide adsorbed on the Ru(001)-p(1×2)-O surface, it is convenient to consider three different regimes of coverage and temperature. First, submonolayer coverages below 260 K give rise to molecularly chemisorbed formamide. Second, annealing to over 260 K results in the decomposition of molecularly chemisorbed formamide to a stable surface intermediate, which decomposes at a higher temperature. Note that this reaction coincides very nearly with the observed desorption of H_2 at 265 K and the desorption of molecular formamide at 255 K. Third, large formamide exposures below 210 K result in the condensation of formamide multilayers. These three cases will be discussed separately below. It is important to note that for all submonolayer coverages, EEL spectra collected after annealing to a given temperature are very similar for formamide on Ru(001)-p(1×2)-O. Thus, the same surface species are formed independent of coverage, although, as the thermal desorption results indicate, the fraction of monolayer formamide that desorbs molecularly *is* a function of coverage. Therefore, only EEL spectra for a low initial formamide exposure (0.5 L) are discussed explicitly without loss of generality.

1. Molecularly Chemisorbed Formamide. Molecularly chemisorbed formamide exists on the Ru(001)-p(1×2)-O surface below 260 K, and there is no evidence for any decomposition of formamide below this temperature. Two different forms of molecularly chemisorbed formamide are observed: a low-temperature form

(22) Pfnür, H.; Menzel, D.; Hoffmann, F. M.; Ortega, A.; Bradshaw, A. M. *Surf. Sci.* **1980**, *93*, 431.

(23) (a) Anton, A. B.; Avery, N. R.; Toby, B. H.; Weinberg, W. H. *J. Electron Spectrosc. Relat. Phenom.* **1983**, *29*, 181. (b) Anton, A. B.; Avery, N. R.; Madey, T. E.; Weinberg, W. H. *J. Chem. Phys.* **1986**, *85*, 507.

(24) (a) Thomas, G. E.; Weinberg, W. H. *Phys. Rev. Lett.* **1978**, *41*, 958. (b) Thiel, P. A.; Weinberg, W. H.; Yates, J. T., Jr. *J. Chem. Phys.* **1979**, *71*, 1643. (c) Thiel, P. A.; Weinberg, W. H.; Yates, J. T., Jr. *Chem. Phys. Lett.* **1979**, *67*, 403. (d) Thiel, P. A.; Weinberg, W. H. *J. Chem. Phys.* **1980**, *73*, 4081. (e) Schwalke, U.; Weinberg, W. H., in preparation.

(25) (a) Schwalke, U.; Parmeter, J. E.; Weinberg, W. H. *J. Chem. Phys.* **1986**, *84*, 4036. (b) Schwalke, U.; Parmeter, J. E.; Weinberg, W. H. *Surf. Sci.* **1986**, *178*, 625.

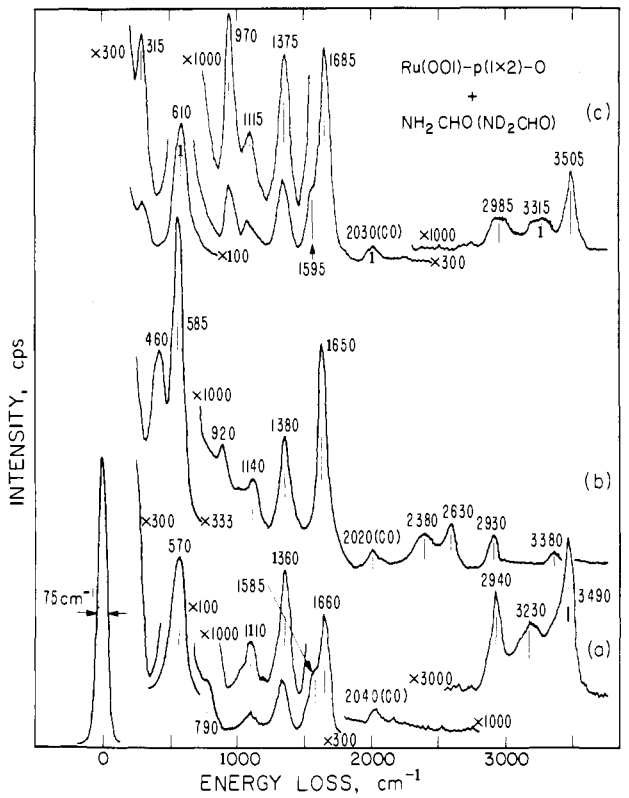

Figure 6. The EEL spectra that result when the **Ru**(001) surface at 80 K is exposed to (a) 0.5 L of NH_2CHO at 80 K, (b) 0.5 L of ND_2CHO at 80 K, and (c) 0.5 L of NH_2CHO at 80 K followed by momentary annealing to 225 K. Corresponding EEL spectra for any given exposure are virtually identical, provided the exposure is not large enough to condense formamide multilayers.

that predominates below approximately 225 K, and a high-temperature form that predominates above 225 K. The conversion between these two forms is a function of temperature only. Note that the conversion temperature coincides with the 225 K formamide thermal desorption peak, suggesting that at high coverage the low-temperature form undergoes competing desorption and conversion to the high-temperature form.

Figue 6a shows the EEL spectrum that results when the Ru(001)-p(1×2)-O surface at 80 K is exposed to 0.5 L of formamide (NH_2CHO). This EEL spectrum is characteristic of the low-temperature form of molecularly chemisorbed formamide. The mode assignments are reasonably straightforward and are listed in Table I, along with data for liquid-[26] and gas-phase[27] formamide. The vibrational modes identified most easily and umambiguously are $\nu_a(NH_2)$, $\nu_s(NH_2)$, ν(CH), ν(CO), and $\delta(NH_2)$, which occurs at 3490, 3230, 2940, 1660, and 1585 cm^{-1}, respectively. The mode at 1360 cm^{-1} is assigned to the overlapping ν(CN) and δ(CH) modes. The modes at 1110 and 790 cm^{-1} are assigned, in accordance with the data for liquid formamide, as being due to the $\rho(NH_2)$ and $\omega(NH_2)$ modes, respectively. The $\nu(NH_2)$ and π(CH) modes are not resolved, although a shoulder on the low-energy side of the $\rho(NH_2)$ mode might be due to π(CH). The intense broad peak (fwhm $\approx$ 125 cm^{-1}) at 570 cm^{-1} is due to the overlap of the δ(NCO) mode of chemisorbed formamide at approximately 525 cm^{-1} [28] and ν_s(RuO) of the p(1×2)-O overlayer at 585 cm^{-1}. Comparison of this mode to the ν_s(RuO) modes of Figure 3, 6b, and 7 (fwhm = 75 cm^{-1} for these features) shows that it is indeed much broader than it would be if only ν_s(RuO) were involved. In some spectra measured after adsorption at 80 K, and in all spectra measured following annealing to 200 K, the weak ν_s-(Ru-NH_2CHO) mode is resolved near 300 cm^{-1}, although it is not resolved in spectrum a in Figure 6 due to the relatively poor elastic peak cutoff. Finally, the weak feature at 2040 cm^{-1} is due to a very small amount (<0.01 monolayer) of coadsorbed CO. This CO is adsorbed from the chamber background and is *not* the result of formamide decomposition. This mode disappears from the EEL spectra following annealing to 400 K, indicating that the desorption of this CO corresponds to the 385 K shoulder in the CO thermal desorption spectrum of Figure 5a.

Figure 6b shows the EEL spectrum which results following a 0.5-L exposure of ND_2CHO to the Ru(001)-p(1×2)-O surface at 80 K. Although some NDHCHO contamination is present in this spectrum (as evidenced by a loss feature at 3380 cm^{-1}), the modes of ND_2CHO are assigned easily. These are listed in parentheses in Table I together with the NH_2CHO/ND_2CHO frequency ratios and the corresponding data for liquid formamide. The observed frequency shifts upon N-deuteriation are in excellent agreement with those reported for liquid formamide and confirm the mode assignments given in Table I and discussed in the preceding paragraph. The frequency shift of the δ(NCO) mode upon N-deuteriation is slightly greater than expected, which suggests that this mode may be coupled to one of the ND_2 deformation modes.

Annealing the surface to temperatures between approximately 225 and 260 K results in the formation of the second form of molecularly chemisorbed formamide, the EEL spectrum of which is shown in Figure 6c (for the case of NH_2CHO). The most striking difference between this form of formamide and the low-temperature form is the presence of a rather intense loss feature at 970 cm^{-1}, the appearance of which correlates with the disappearance of the mode at 790 cm^{-1} in Figure 6a. This 970 cm^{-1} loss feature shifts down to 770 cm^{-1} in the case of ND_2CHO (not shown), and the large frequency shift upon N-deuteriation indicates that is must be due to an NH_2 deformation mode. This is assigned to the NH_2 wagging mode of chemisorbed formamide, which is almost certainly adsorbed such that this mode involves motion of the NH_2 hydrogen atoms largely perpendicular to the surface. Figure 6c also shows a rather intense and well-resolved ν(Ru-NH_2CHO) peak at 315 cm^{-1}, in contrast to Figure 6a. The other differences between the EEL spectra of the low- and high-temperature forms of molecularly chemisorbed formamide are minor.

The ν(CO) frequencies of the two forms of molecularly chemisorbed formamide indicate clearly that the CO double bond is maintained in each case. Hence, for both forms, bonding to the surface is via lone pair donor bonds with the oxygen and/or nitrogen atoms rather than by rehybridization of the CO bond. Since the distinction among η^1(O)-NH_2CHO, η^1(N)-NH_2CHO, and η^2(N,O)-NH_2CHO is difficult, further discussion of the nature of the two forms of molecularly chemisorbed formamide is deferred to Sections III.B.2 and IV.

2. Decomposition of Chemisorbed Formamide. Chemisorbed formamide of the type characterized by the EEL spectrum of Figure 6c remains on the Ru(001)-p(1×2)-O surface to approximately 260 K, at which temperature conversion to another species occurs. This conversion coincides both with the highest temperature (255 K) molecular formamide thermal desorption peak and with the low-temperature H_2 thermal desorption peak. Consequently, the high-temperature form of molecularly chemisorbed formamide undergoes competing desorption and decomposition, just as the form present at lower temperatures undergoes competing desorption and conversion to the high-temperature form. The surface species formed at 260 K is stable to 420 K, and its decomposition, as monitored by EELS, coincides with the CO and H_2 thermal desorption peaks shown in Figure 5. On the basis of the EEL spectra of Figure 7, this new species is identified as η^2(N,O)-NHCHO [cf. Figure 2, structure **4**]. This species is analogous to the η^2(O,O)-OCHO (η^2-formate) formed from formic acid decomposition on both Ru(001) and a number of other metal surfaces.[4] The vibrational modes of η^2-NHCHO are assigned and compared with those of related organometallic compounds[12c] and

(26) Suzuki, I. *Bull. Chem. Soc. Jpn.* **1960**, *33*, 1359.
(27) (a) Evans, J. C. *J. Chem. Phys.* **1954**, *22*, 1228. (b) King, S. T. *J. Phys. Chem.* **1971**, *75*, 405.
(28) The frequency of 525 cm^{-1} for δ(NCO) is obtained from EEL spectra of NH_2CHO adsorbed on hydrogen presaturated Ru(001) at 80 K, where the same molecular formamide species is formed but there is no overlapping ν_s(RuO) mode.

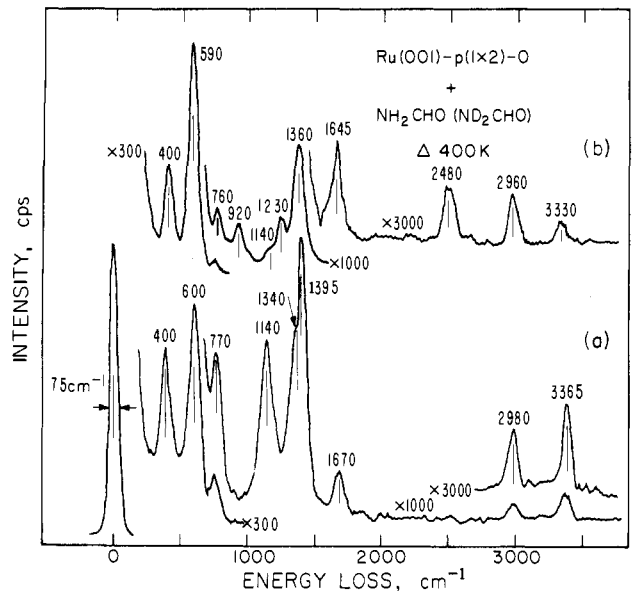

Figure 7. The EEL spectra that result when the Ru(001)-p(1×2)-O surface at 80 K is exposed to (a) 0.5 L of NH_2CHO at 80 K and (b) 0.5 L of ND_2CHO at 80 K and annealed momentarily to 400 K. These spectra are characteristic of η^2(N,O)-NHCHO and η^2(N,O)-NDCHO.

Table II. Vibrational Modes and Assignments for η^2(N,O)-NHCHO on the Ru(001)-p(1×2)-O Surface[b]

mode	η^2(N,O)-NHCHO (η^2(N,O)-NDCHO, ratio), Ru(001)-p(1×2)-O	η^2-formate; Ru(001) (**4a,b**)[a]	[$R_2MN(CH_3)$-$C(CH_3)O]_2$ (**12c**)
ν(NH)	3365 (2480, 1.36) w		
ν(CH)	2980 (2960, 1.01) w	2920 w	
ν_a(NCO)[a]	n.o. (n.o.)	n.o.	1571–1585 st
ν_s(NCO)[a]	1395 (1360, 1.03) st	1360 st	1392–1400 st
δ(NH)	n.o. (1230) m		
π(NH)	1140 (920, 1.24) m		
δ(CH)	1340 (n.o.) sh	n.o.	
π(CH)	n.o. (n.o.)	n.o.	
δ(NCO)[a]	770 (760, 1.01) m	805 m	n.o.
ν(M ligand)	400 (400, 1.00) st	380 st	363–492 st

[a] In the case of η^2-formate, these skeletal modes are obviously OCO modes rather than NCO modes. [b] Vibrational frequencies for η^2-NDCHO and the corresponding η^2-NHCHO/η^2-NDCHO frequency ratios are listed in parentheses. Data for η^2(O,O)-OCHO (η^2-formate) and for the compounds $[R_2MN(CH_3)C(CH_3)O]_2$ (M = Ga or In, R = CH_3 or CH_2CH_3) are given for comparison. All frequencies are in cm^{-1}. s = symmetric, a = asymmetric, st = strong, m = medium, w = weak, sh = shoulder, n.o. = not observed.

to those of η^2-formate on Ru(001)[4a,b] in Table II. Figure 7b shows the EEL spectrum of η^2(N,O)-NDCHO formed from ND_2CHO decomposition, and the vibrational frequencies of this species are listed in parentheses in Table II.

The identification of the species represented by the EEL spectrum of a of Figure 7a as η^2-NHCHO follows from the presence of single ν(NH) and ν(CH) modes, the lack of a $\delta(NH_2)$ mode near 1580 cm^{-1}, the lack of a strong carbonyl ν(CO) mode in the range 1500–1800 cm^{-1}, and the similarity of its skeletal modes to those of both η^2-formate on Ru(001)[4a,b] and the related organometallic compounds of the type shown below[12c]

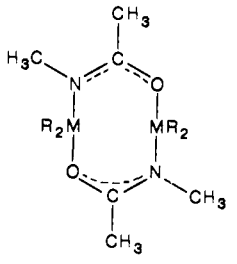

M = Ga or In; R = CH_3 or C_2H_5

Note especially the close agreement between the ν_s(NCO) modes of η^2-NHCHO and the η^2-$N(CH_3)C(CH_3)O$ complexes and between the δ(NCO) [δ(OCO)] and ν(Ru–NHCHO) [ν(Ru–OCHO)] modes of η^2-NHCHO and η^2-formate. The increase in the frequency of δ(NCO) in going from gas-phase formamide to η^2(N,O)-NHCHO (565 to 770 cm^{-1}) is similar to the frequency increase of δ(OCO) in going from gas-phase formic acid to η^2-formate on Ru(001) (625 to 805 cm^{-1}) and is indicative of delocalized π-bonding within the NCO group. The EEL spectrum of η^2-NDCHO also helps to confirm the assignment of the modes observed at 1395, 770, and 400 cm^{-1} in the EEL spectrum of η^2-NHCHO, since none of these modes shifts significantly upon N-deuteriation. A weak peak which occurs between 1630 and 1680 cm^{-1} may or may not be due partially to the ν_a(NCO) mode of η^2-NHCHO. Since this peak also appears in EEL spectra after annealing to over 420 K, which has caused the stronger modes of η^2-NHCHO to disappear, it must be attributed primarily to a small amount of molecularly chemisorbed formamide that has readsorbed from the chamber background. The frequency of this mode is somewhat higher than the frequencies of the ν_a(NCO) modes in the related gallium and indium complexes, although the ν_a(NCO) modes of a similar series of aluminum complexes are somewhat closer, ranging from 1580 to 1621 cm^{-1}.[12b] Thus, the ν_a(NCO) mode may be partially responsible for the loss feature appearing at 1670 cm^{-1}, or it may be simply too weak to be observed. Note that this mode should not be strictly dipolar-forbidden in the case of η^2-NHCHO, unlike ν_a(OCO) in η^2-formate.

The assignment of the CH and NH in-plane (δ) and out-of-plane (π) bending modes is less straightforward than the assignment of the skeletal, frustrated translational, CH stretching, and NH stretching modes. The shoulder at 1340 cm^{-1} in Figure 7a is quite reproducible and is assigned as δ(CH), in good agreement with the δ(CH) frequency of 1377 cm^{-1} in sodium formate.[29] This mode is not resolved in the case of η^2-NDCHO due to the slight downshift of the ν_s(NCO) mode to 1360 cm^{-1}. The mode at 1140 cm^{-1} in η^2-NHCHO is downshifted to 920 cm^{-1} in η^2-NDCHO and is thus assigned as an NH bending mode, although without vibrational data for η^2-NHCHO complexes it is not obvious whether this is the π(NH) or δ(NH) mode. The frequency of 1140 cm^{-1} seems more reasonable for the π(NH) mode, whereas the relatively strong intensity of the peak corresponding to this mode in Figure 7a would seem suggestive of the δ(NH) mode (see Section IV.B). The weak feature at 1140 cm^{-1} in Figure 7b is probably due to the presence of η^2-NHCHO as an impurity in η^2-NDCHO; note also the ν(NH) loss peak at 3330 cm^{-1} in this spectrum. The peak at 1230 cm^{-1} in Figure 7b is probably due to δ(ND) which is upshifted and not resolved from ν_s(NCO) in the case of η^2-NHCHO [which suggests further that the NH bend at 1140 cm^{-1} is indeed π(NH)]. This would require an anomalously small frequency shift of the δ(NH) mode upon deuteriation ($\leq$1.18), a condition which could be satisfied if this mode couples to the ν_a(NCO) mode.[30] No mode is observed that can be clearly attributed to π(CH), although this mode could contribute to the intensity of the 1140-cm^{-1} feature in either spectrum of Figure 7. The preferred mode assignments for the CH and NH bending modes are listed in Table II. Despite some uncertainty in the detailed assignment of the CH and NH bending modes, the identification of η^2(N,O)-NHCHO can be made unambiguously on the basis of the other observed vibrational modes. Other formamide-derived ligands that have been identified in organometallic chemistry can be eliminated easily on the basis of the observed EEL spectra (cf. Section IV.B).

Upon annealing to 420 K, the modes due to η^2-NHCHO disappear, leaving only the characteristic features of the p(1×2)-O

(29) Nakamoto, K. *Infrared and Raman Spectra of Inorganic and Coordination Compounds*, 3rd ed.; Wiley & Sons: New York, 1978; pp 231–233.

(30) Coupling between ν_a(NCO) and δ(NH) is possible for η^2-NHCHO since both of these modes are of the same symmetry and are expected to occur in the same frequency range. Such coupling could lead to very different intensities for δ(NH) in η^2-NHCHO and δ(ND) in η^2-NDCHO, as well as an anomalously small frequency shift for this mode upon N-deuteriation.

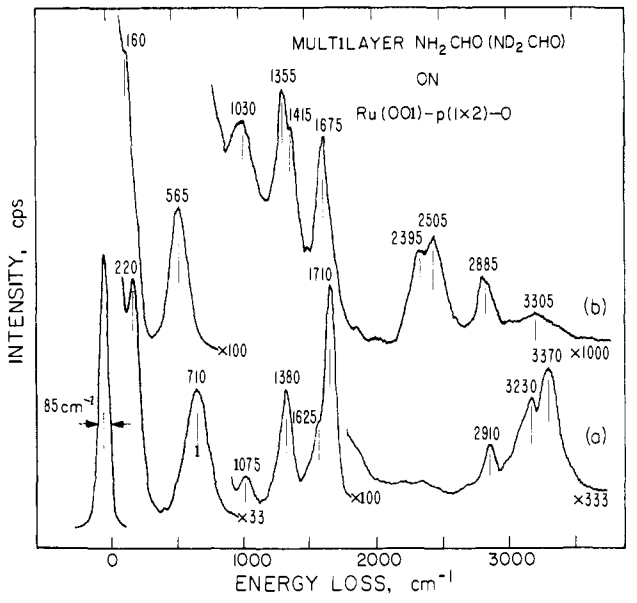

Figure 8. The EEL spectra that result when the Ru(001)-p(1×2)-O surface at 80 K is exposed to (a) 10 L of NH_2CHO and (b) 10 L of ND_2CHO, showing the characteristic features of formamide multilayers.

Table III. Vibrational Frequencies and Mode Assignemnts for Multilayer NH_2CHO and ND_2CHO on the Ru(001)-p(1×2)-O Surface[a]

mode	NH_2CHO	ND_2CHO	mode	NH_2CHO	ND_2CHO
$\nu_a(NH_2)$	3370	2505	$\delta(NH_2)$	1625	
$\nu_s(NH_2)$	3230	2395	$\rho(NH_2)$	1075	1030
$\nu(CH)$	2910	2885	$\pi(CH)$		
$\nu(CO)$	1710	1675	$\omega(NH_2)$	710	565
$\delta(CH)$	1380	1415	$\delta(NCO)$	n.o.	n.o.
$\nu(CN)$		1355	lattice[a]	220	160

[a] Probably coupled to $\tau(NH_2)$. [b] All frequencies are in cm^{-1}. For corresponding frequencies of liquid formamide, see Table I.

overlayer (and a weak mode near 1650 cm^{-1} due to readsorbed formamide) in subsequent EEL spectra. Since the TDMS results indicate that CO and H_2 are evolved from the surface at 420 K, it can be concluded that both of these desorption products result from η^2-NHCHO decomposition and that only nitrogen adatoms remain on the Ru(001)-p(1×2)-O surface above 420 K. Nitrogen adatoms are not detected by EELS because the ν_s(RuN) mode is obscured by the ν_s(RuO) mode of the p(1×2)-O overlayer (note that $\theta_O \sim 10\theta_N$). However, the presence of nitrogen adatoms above 420 K is confirmed by the recombinative desorption of N_2 that is observed near 570 K. Thus the decomposition products of η^2-NHCHO on Ru(001)-p(1×2)-O are N(a), H_2(g), and CO(g).

3. Formamide Multilayers. Molecular multilayers of formamide condense on the Ru(001)-p(1×2)-O surface when this surface at 80 K is exposed to approximately 7 L or more of formamide. The multilayers desorb at 210 K, and EEL spectra measured after annealing to temperatures in the range of 80–200 K are identical. Multilayer EEL spectra are shown in Figure 8 for both NH_2CHO and ND_2CHO, and the observed vibrational modes are listed in Table III. It may be seen by comparison of Tables I and III that, in general, the vibrational modes of the formamide multilayers are even closer to those of liquid formamide than are those of the low-temperature form of chemisorbed formamide. Two extremely intense loss features are characteristic of the NH_2CHO (ND_2CHO) multilayers: a lattice mode at 220 (160) cm^{-1} (that may couple to the NH_2 twisting mode which occurs at 200 cm^{-1} in liquid NH_2CHO) and the NH_2 wagging mode at 710 (565) cm^{-1}. This latter mode and the NH_2 stretching modes are quite broad, indicative of considerably hydrogen bonding within the multilayers. The NH_2 (ND_2) asymmetric stretch is downshifted by approximately 120 cm^{-1} compared with that of the chemisorbed formamide at 80 K. For NH_2CHO multilayers, the peak at 1380 cm^{-1} is assigned to the overlapping δ(CH) and ν(CN) modes, while the peak at 1075 cm^{-1} is assigned to the overlapping π(CH) and $\rho(NH_2)$ (rocking deformation) modes. In both case, the frequencies observed are intermediate between those of the two constituent bands in liquid NH_2CHO. For ND_2CHO multilayers, the ν(CN) and δ(CH) modes are resolved and occur at 1355 and 1415 cm^{-1}, respectively, and the broad feature centered at 1030 cm^{-1} is due to the overlapping $\delta(ND_2)$, π(CH), and $\rho(ND_2)$ modes [and perhaps some intensity is derived also from the overtone of the $\omega(ND_2)$ mode]. Note that the loss feature centered at 3305 cm^{-1} indicates that once again some NDHCHO or NH_2CHO impurity is present in the ND_2CHO.

IV. Discussion

A. Molecularly Chemisorbed Formamide. The EEL spectra a and c of Figure 6 indicate clearly the presence of two slightly different forms of chemisorbed formamide on the Ru(001)-p(1×2)-O surface below 260 K. Since the observed CO stretching frequencies show that extensive rehybridization of the CO bond does not occur in either case (i.e., the CO double bond is maintained), bonding to the surface must occur via an electron lone pair on either the oxygen or nitrogen atom, or possibly via electron lone pairs on both of these atoms. Thus, there are three distinct, possible bonding configurations, corresponding to structures I, II, and III of Figure 1. In all three of these configurations, the bonding may be thought of in simple Lewis acid–base terms, with the formamide molecule acting as the Lewis base and the surface as the Lewis acid.

The distinction among these three forms of molecularly chemisorbed formamide is not trivial. It is conceivable that two of these three forms could coexist on the surface below 225 K, with desorption of the more weakly bound form occurring at this temperature. However, the sudden appearance of the rather intense 970-cm^{-1} mode when the surface is annealed to 225 K, coupled with the lack of any evidence for two different formamide species in Figure 6a, indicates that a conversion from one formamide species to another is occurring at 225 K. The most likely scenario is one in which chemisorbed formamide of type I or II is converted to the more strongly bound, bidentate species III. This model is especially appealing intuitively since η^2(N,O)-NH_2CHO is the logical intermediate to the η^2(N,O)-NHCHO formed at 260 K. In addition, it is quite possible that the conversion of I or II to III would require some desorption of I or II at high coverages, as is observed, for electronic reasons. This effect of competing desorption and conversion to a more highly coordinated species has been observed previously for other metal–adsorbate systems.[31]

It is likely for several reasons that the low-temperature form of molecularly chemisorbed formamide is η^1(O)-NH_2CHO. First, it is well-known that the oxygen atom of formamide is much more basic than the nitrogen atom in homogeneous organic chemistry.[32] It thus seems reasonable to expect that the oxygen atom would be more basic (in the Lewis sense) with respect to bonding to a metal surface. Second, data from a study of the N-bonded and O-bonded isomers of $(NH_3)_5Co(NH_2CHO)^{3+}$ suggest that O-bonded amides are more stable in organometallic compounds than N-bonded amides.[33] It was found that the N-bonded form of $[(NH_3)_5Co(NH_2CHO)](ClO_4)_3$ isomerizes to the O-bonded form in the solid state. It was also found that heating $[(NH_3)_5Co(H_2O)](ClO_4)_3$ in *N,N*-dimethylformamide produced only the O-bonded isomer of $(NH_3)_5Co(NMe_2CHO)_3^{+}$. Third, the ν(CO) frequency of 1660 cm^{-1} for the low-temperature form of molecularly chemisorbed formamide is somewhat reduced from the gas-phase value of 1734 cm^{-1}, and similar decreases in ν(CO) have been observed previously for η^1(O)-acetone[5a] and η^1(O)-formaldehyde[6b] on oxygen-precovered Ru(001) surfaces. On the other hand, infrared data for η^1(N)-NHCRO complexes (cf. Figure 2, structure **2**) show that in all cases the frequency of ν(CO) is greater than 1700 cm^{-1},[10] and we would expect ν(CO) to be similarly high

(31) See, for example, Avery, N. R. (*Surf. Sci.* **1984**, *137*, L109) as well as ref 6b and 7a.
(32) Streitwieser, A., Jr.; Heathcock, C. H. *Introduction to Organic Chemistry*; Macmillan: New York, 1976; pp 466–467.
(33) Balahura, R. J.; Jordan, R. B. *J. Am. Chem. Soc.* **1970**, *92*, 1533.

for an η^1(N)-formamide in which the formamide oxygen atom does not interact directly with the surface. Finally, an η^1(O)-NH_2CHO would be expected to maintain a nearly planar structure (gas-phase formamide has a planar structure), and the NH_2 wagging vibration would involve motion of the NH_2 hydrogen atoms out of this plane and largely parallel to the surface. Hence, the $\omega(NH_2)$ mode would be expected to maintain a nearly planar structure (gas-phase formamide has a planar structure), and the NH_2 wagging vibration would involve motion of the NH_2 hydrogen atoms out of this plane and largely parallel to the surface. Hence, the $\omega(NH_2)$ mode would be expected to be rather weak in specular EEL spectra, as observed in Figure 6a. On the other hand, η^1(N)-NH_2CHO should result in a more intense NH_2 wagging mode, since the NH_2 group will no longer be in (or nearly in) a plane perpendicular to the surface; and this mode will involve motion of the NH_2 hydrogen atoms largely perpendicular to the surface. Taken together, these arguments provide a strong case for the low-temperature form of molecularly chemisorbed formamide being η^1(O)-NH_2CHO.

For the reasons discussed above, and because of the appearance of an intense $NH_2(ND_2)$ wagging mode at 970 (770) cm^{-1}, it is very likely that the high-temperature form of molecularly chemisorbed formamide is η^2(N,O)-NH_2CHO. Indeed, the large upshift in the frequency of $\omega(NH_2)$ from 790 to 970 cm^{-1} in going from the low- to the high-temperature form is in itself suggestive of N-coordination to the surface. The other observed NH_2 modes of molecularly chemisorbed formamide are not shifted greatly upon N-coordination because they do not involve motion of the NH_2 hydrogen atoms directly toward the surface, which in the case of $\omega(NH_2)$ increases the restoring force associated with this vibration and results in the large frequency increase. A similar phenomenon occurs with the $\delta_s(NH_3)$ mode of ammonia when this molecule adsorbs on metal surfaces,[2] and the frequency of this mode shifts from 950 cm^{-1} in the gas phase to approximately 1150 cm^{-1}. The fact that the conversion of η^1(O)-NH_2CHO to η^2(N,O)-NH_2CHO occurs only when the surface is annealed to 225 K indicates that an activation energy of approximately 13 kcal mol^{-1} is associated with this conversion. This activation barrier is probably associated with the partial rotation of the NH_2 group about the CN bond, and the distortion of the NH_2 group which the formamide molecule must undergo in order for the nitrogen atom to coordinate to the surface. As stated previously, the η^1(O)-NH_2CHO probably maintains the planar structure of gas-phase formamide, for which the activation barrier to rotation of the NH_2 group about the CN bond has been measured to be 18 kcal·mol^{-1}.[34] In η^2(N,O)-NH_2CHO, however, the nitrogen is expected to obtain an approximately tetrahedral bonding geometry, with the hydrogen atoms of the NH_2 group disposed symmetrically about, but no longer in, the OCN plane (cf. Figure 1, structure III). Thus, the plane containing the NH_2 group must rotate approximately 90° about the CN bond and the NH bonds must tilt away from the surface in order for the nitrogen atom to approach the surface in the proper orientation.

While the molecular formamide thermal desorption peak at 255 K is undoubtedly due to desorption from the monolayer, the desorption peak at 225 K could be attributed either to monolayer or second-layer desorption. The fact that this lower temperature desorption peak occurs at the same temperature as the conversion of the low-temperature form of chemisorbed formamide to the high-temperature form suggests that this is a monolayer desorption state, while the proximity of the 225 K desorption peak to the multilayer desorption peak at 210 K might suggest that it results from second-layer desorption. (The low-temperature form of chemisorbed formamide identified by EELS is clearly not second-layer formamide, since it is present even following very low initial exposures). While there is precedent for resolving second-layer thermal desorption features in thermal desorption spectra, such features were not resolved in the case of η^1(O)-bonded formaldehyde[6] or acetone[5] on oxygen-precovered Ru(001) surfaces. We thus favor (slightly) the assignment of the 225 K thermal desorption feature as a monolayer desorption state.

B. Formamide Decomposition. It has been shown that the high-temperature form of molecularly chemisorbed formamide decomposes near 260 K with H_2 evolution to produce η^2(N,O)-NHCHO with some molecular desorption occurring for sufficiently high coverages. The η^2-NHCHO would be of C_s symmetry if all five of its atoms were located in a plane perpendicular to the Ru(001)-p(1×2)-O surface and of C_1 symmetry if this is not the case. According to the surface dipole selection rule, eight vibrational modes should be observed in specular EEL spectra for C_s symmetry:[35] ν(NH), ν(CH), ν_a(NCO), ν_s(NCO), δ(CH), δ(NH), δ(NCO), and ν(Ru–NH_2CHO). (Note, however, that this does *not* imply that all of these modes are dipolar in nature.) For C_1 symmetry, all of these modes should be dipole-allowed in specular EEL spectra, and, in addition, the π(CH) and π(NH) modes should also be dipole-allowed. However, it is possible that not all dipole-allowed modes will be observed in specular EEL spectra because some modes may be intrinsically weak and/or accidentally degenerate with stronger modes; and for C_s symmetry it is possible that the dipole-forbidden π(NH) and π(CH) modes could be observed (but probably very weakly) in specular EEL spectra due to scattering via nondipolar (i.e., impact) mechanisms. As an example of the former possibility, note that no ν_a(NCO) mode is identified conclusively for η^2-NHCHO even though this mode is technically dipole-allowed for either C_s or C_1 symmetry. Since the identification of η^2-NHCHO as having either C_s or C_1 symmetry hinges on the dipole activity of the π(NH) and π(CH) modes, and since neither of these modes can be assigned with complete confidence, the symmetry of η^2-NHCHO must be regarded as uncertain. If the mode at 1140 (920) cm^{-1} in the case of η^2-NHCHO (η^2-NDCHO) is indeed π(NH), then this would be strong evidence for C_s symmetry, since off-specular EEL spectra indicate that this mode is largely dipolar in nature. This is contrary to our expectation, however, that η^2-NHCHO should be planar, just as η^2-formate is planar.

Another important question regarding the structure of η^2-NHCHO on the Ru(001)-p(1×2)-O surface is whether this species is chelating or bridging, i.e., is it bonded to only one ruthenium atom or to at least two ruthenium atoms?

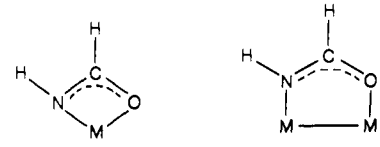

Organometallic analogues are known for both the chelating and bridging structures shown above.[12] Analogous organometallic compounds are also known for chelating and bridging η^2-formates, and these may be distinguished from one another by the frequency difference between the ν_a(OCO) and ν_s(OCO) modes.[29] However, since the ν_a(NCO) mode is not identified positively for η^2-NHCHO on Ru(001)-p(1×2)-O, this criterion cannot be used to establish whether the η^2-NHCHO is bridging or chelating. Nevertheless, it is extremely likely that the η^2-NHCHO is bridge-bonded for three reasons. First, the strong ν_s(NCO) mode of η^2-NHCHO on Ru(001)-p(1×2)-O, occurring at 1395 cm^{-1}, is in perfect agreement with the ν_s(NCO) modes observed for bridging $N(CH_3)C(CH_3)O$ species in the gallium and indium compounds referenced in Table II, while a series of chelating η^2-NArCHO (Ar = aryl) species in rhenium, ruthenium, and osmium compounds have ν_s(NCO) modes that are more than 100 cm^{-1} lower in frequency, ranging from 1250 to 1290 cm^{-1}.[12a,b] Second, η^2(N,O)-NRCHO ligands that have been identified in organometallic compounds are chelating only in mononuclear metal compounds and bridging in polynuclear metal compounds,[12] and the behavior of the surface with respect to ligand bonding should be more similar to that of the polynuclear metal compounds. Third, all η^2-formates identified previously on metal surfaces which

(34) Reference 32, p 452.

(35) Reference 15, see chapters 1 and 3.

have been assigned structures have been identified as bridging rather than chelating.[4]

Although it has been shown that the EEL spectra of Figure 7 are fully consistent with an η^2(N,O)-NHCHO species, it is instructive to consider briefly other plausible species that might be formed from formamide decomposition on the Ru(001)–p(1×2)–O surface and to eliminate them on the basis of these EEL spectra. Although all of the species depicted in Figure 2 have analogues in organometallic chemistry, it can be shown easily that all but η^2(N,O)-NHCHO are inconsistent with the EEL spectra of Figure 7. Species **1**, **3**, **5a**, and **5b** lack CH bonds, a fact that in itself is sufficient to eliminate them from consideration. (The rather sharp peak at 2980 cm^{-1} in the EEL spectrum of Figure 7a is much too narrow to be due to a hydrogen-bonded NH or OH stretching mode, and the frequency of this mode does not shift significantly upon N-deuteriation.) Species **1**, **2**, **5a**, and **5b** contain CO or CN double bonds which, based on the organometallic studies cited in Section I, should give rise to intense stretching modes near 1500–1650, 1700–1750, 1600, and 1775 cm^{-1}, respectively. Species **1**, **3**, and **5b** contain NH_2 groups, which is inconsistent with the lack of a $\delta(NH_2)$ mode, the presence of only a single ν(NH) peak in Figure 7a, and the observed desorption of H_2 at 265 K. Species **1**, **2**, **5a**, and **5b** contain well-defined single and double skeletal bonds and should thus have δ(NCO) frequencies similar to those of gas-phase formamide or formic acid (565 and 625 cm^{-1}), rather than near 800 cm^{-1} as for the case of η^2-formate on Ru(001). Species **5a** contains an OH group, and there is no spectroscopic evidence for the formation of either free [ν(OH) > 3500 cm^{-1}] or hydrogen-bonded [ν(OH) lowered and broadened] OH bonds in Figure 7a. Thus all the species depicted in Figure 2 except η^2(N,O)-NHCHO are inconsistent with the EEL spectra of Figure 7. On the other hand, the η^2(N,O)-NHCHO is completely consistent with both the EEL spectra and the TDMS results.

It is interesting to compare the products observed in η^2-NHCHO decomposition to those observed in η^2-formate decomposition on Ru(001). The η^2-formate decomposes via two competing mechanisms near 350 K, one of which produces adsorbed CO and atomic oxygen and the other evolving gaseous CO_2:[4a,b]

$$\eta^2\text{-HCOO(a)} \rightarrow \text{H(a)} + \text{O(a)} + \text{CO(a)}$$
$$\rightarrow \text{H(a)} + \text{CO}_2\text{(g)}$$

The decomposition of η^2-NHCHO to H_2(g), N(a), and CO(g) is analogous to the first of these reactions, although in this case the H_2 and CO that are evolved are reaction-limited desorption products since neither carbon monoxide nor hydrogen is adsorbed on the Ru(001)–p(1×2)–O surface at the temperature of η^2-NHCHO decomposition. The decomposition of η^2-NHCHO to HNCO(g) and $^1/_2H_2$(g) would be analogous to the second formate decomposition reaction, but it is not observed.

Finally, it should be emphasized that there is no evidence for any direct interaction or chemical reaction between the oxygen adatoms of the p(1×2)–O overlayer and formamide or its decomposition products. There is no desorption of H_2O, NO, or high-temperature (recombinative) CO[36] following formamide adsorption. There is no evidence in any EEL spectra for the formation of OH or NO bonds, and EEL spectra measured after annealing to 700 K show all of the characteristic features of the p(1×2)–O overlayer, which are completely unaffected by the adsorption and decomposition of formamide.

V. Conclusions

Below 260 K, formamide adsorbs molecularly on the Ru(001)–p(1×2)–O surface. Two different forms of molecularly chemisorbed formamide are observed: a low-temperature form below 225 K and a high-temperature form between 225 and 260 K. The low-temperature form bonds to the surface via an oxygen electron lone pair only, while the high-temperature form bonds to the surface through lone pairs on both the oxygen and the nitrogen atoms. For sufficiently high coverages, the conversion at 225 K is accompanied by some desorption of molecular formamide. Molecular multilayers of formamide may be condensed on the Ru(001)–p(1×2)–O surface at temperatures below 210 K.

At 260 K, the high-temperature form of molecularly chemisorbed formamide undergoes NH bond cleavage and converts to a bridging η^2(N,O)-NHCHO species. This conversion is accompanied by molecular formamide desorption if a sufficiently high coverage is involved. The η^2-NHCHO decomposes at 420 K, yielding adsorbed nitrogen adatoms and evolving H_2 and CO. The nitrogen adatoms recombine and desorb near 600 K, leaving the p(1×2)–O overlayer intact. For a saturation formamide coverage, approximately 0.05 monolayer of η^2-NHCHO forms and decomposes.

Acknowledgment. Principal support of this work was provided by the National Science Foundation under Grant No. CHE-8516615. Acknowledgment is also made to the donors of the Petroleum Research Fund, administered by the American Chemical Society, for partial support.

Registry No. Ru, 7440-18-8; O, 17778-80-2; formamide, 75-12-7.

(36) Carbon monoxide formed from the recombinative desorption of carbon and oxygen adatoms on Ru(001) desorbs in the temperature range of 550–700 K. Hills, M. M.; Parmeter, J. E.; Weinberg, W. H. *J. Am. Chem. Soc.* **1987**, *109*, 4224.